DOI:10.13476/j.cnki.nsbdqk.2020.0111
娄伟,李致家,刘玉环.多模式下泾河上游流域未来降水变化预估[J].南水北调与水利科技(中英文),2020,18(6):01-16. LOU W,LI Z J,LIU Y H. Projection of future precipitation changes in upper Jinghe River basin using multiple models [J]. South-to-North Water Transfers and Water Science & Technology,2020,18(6):01-16. (in Chinese)

多模式下泾河上游流域未来降水变化预估

娄伟,李致家,刘玉环

(河海大学 水文水资源学院,南京 210098)

摘要:利用站点实测资料、GCMs 月数据对 GCMs 进行秩评分评估排序,从 21 种 GCMs 模式优选出的 6 种 GCM 模式的日数据、6 种 GCM 集成的气候模式、站点实测资料和 NCEP 再分析资料构建统计降尺度模型 SDSM,预估泾河上游流域的未来降水变化。结果表明:构建的降尺度模型对降水模拟较为可靠,率定期各模式决定系数 R^2 为 0.228~0.324,标准误差为 0.354~0.450,率定期和验证期模拟月均降水与实测值年内分布相近。在降尺度性能评价中集成模式表现最好。在 RCP 4.5 情景下,泾河上游流域未来降水大多数模式和集成模式呈增加趋势,到 2030 年泾河上游流域降水量将增加 4.8%,且当地的春季雨量会增加,夏季雨量会减少。

关键词:气候变化;降水;秩评分评估;统计降尺度;泾河上游流域

中图分类号:P338;TV213 **文献标志码**:A **开放科学(资源服务)标志码(OSID)**:

泾河是黄河的二级支流,也是黄河十大水系之一,年平均降水量 350~600 mm,属于半湿润半干旱过渡地区[1]。泾河上游三关口流域位于黄土高原西部宁南山区,由于气候变化的影响,当地的水土流失、水资源短缺等问题越来越突出,已成为阻碍当地经济发展的瓶颈,所以定性定量地研究未来气候变化对泾河上游地区水资源的影响很有必要。

目前,较为普遍的研究区域未来气候变化的一种方法是利用全球气候模型的输出数据(global climate models,GCMs)结合不同的降尺度方法来预测区域未来气候的变化情景,GCM 能够更好地模拟大尺度气候信息中最重要的平均特征,所以在气候变化对水文水资源的影响研究中,这种方法得到了广泛应用[2-7]。降尺度方法可分为 3 类:统计降尺度、动力降尺度以及统计—动力相结合的方法,每种方法都各有优劣,其中统计降尺度方法 SDSM(statistical downscaling model)具有不需考虑边界条件对预测结果的影响、计算量小、模型易于构造等优点,在气候变化研究中得到青睐[8-9]。国内外学者利用 GCM 结合统计降尺度方法对气温和降水进行预测都取得了不错的效果,如:Hasan 等[10]利用 SDSM 结合 GCM 预测了文莱 2017—2076 年的最高气温、最低气温和降水,得到最高气温呈增加趋势,最低气温和降水呈减小趋势;Huang 等[11]和 Liu 等[12]利用统计降尺度方法分别对长江流域和长江中下游地区的未来降水进行了预测,结果表明长江流域的大部分地区将以上升趋势为主;陈鹏翔等[13]基于统计降尺度的多模式集合对中亚春季降水进行了预估,结果表明多模式降尺度集合结果优于大部分单个模式降尺度结果。

本文采用一种基于多目标函数的秩评分方法对 CMIP5 提供的 21 种 GCMs 月降水输出数据进行评估,优选出 6 种 GCM,利用 6 种 GCM 日降水数据驱动 SDSM 模型,进而生成泾河上游流域未来气候变化情景,既可以解决不同 GCM 区域适应性问题减少单个 GCM 模拟的不确定性,又可以提供多模

收稿日期:2020-02-19 **修回日期**:2020-06-03 **网络出版时间**:2020-06-23
网络出版地址:https://kns.cnki.net/kcms/detail/13.1430.TV.20200623.0928.004.html
基金项目:国家自然科学基金(51679061);宁夏重点研发计划(2018BEG02010)
作者简介:娄伟(1996—),男,安徽安庆人,主要从事水文气象与水文预报研究。E-mail:18856329193@163.com
通信作者:李致家(1962—),男,山西运城人,教授,博士,主要从事水文物理规律模拟与预报研究。E-mail:zjli@hhu.edu.cn

式及多模式集合下气候变化区间,从而为当地政府制定更为有效的用水方案、更好地发掘水资源的潜力提供依据。

1　研究方法

1.1　研究区域概况

本文中泾河上游流域是指位于宁夏泾源县内六盘山东侧的三关口水文站以上的控制流域,流域内设有大湾、瓦亭、什字等雨量站,流域附近设有历史气象资料丰富的固原气象站,流域面积有 218 km^2,降水主要集中在 6—9 月[14],该流域处于六盘山东麓,海拔高度在 1 640～2 930 m,属于土石山林区,其夏季受到东南季风的影响,冬季受到蒙古高压的控制,具有显著的大陆性季风气候及高寒山区气候特征。

1.2　数据资料

本研究需要 3 类数据:站点实测降水数据、NCEP 再分析资料和 GCM 模拟的当前与未来气候条件下的输出数据。站点实测降水数据可通过查找相关水文年鉴,得到泾河上游三关口流域内大湾、瓦亭、什字、三关口的 1991—2014 年逐日降水资料。从中国气象数据网得到流域附近固原站 1970—2005 年的月降水资料用于对 GCMs 模式的评价去优选 6 个更贴近当地的 GCM 模式。其中从水文年鉴与中国气象数据网站得到的降水数据的数据精度都为 0.1 mm,故将其放在一起使用。NCEP 再分析资料由美国环境预报中心(NCEP)和国家大气研究中心(NCAR)联合提供,选择时段与实测数据同期(1991—2014 年),包括可降水量、地表平均气温、比湿、相对湿度、风速 u 分量、风速 v 分量等气象资料。GCM 模式资料下载自 CMIP5(https://esgf-node.llnl.gov/projects/cmip5/),相较于之前的气候模式,CMIP5 采用了更为合理的参数化、通量处理方案和耦合器技术,可以得到更为精确和详细的情景数据[15-16]。下载其中 21 个 GCM 模式在 RCP 4.5 情景下的 1970—2005 年月尺度降水输出和优选出的 6 个 GCM 模式在 RCP 4.5 情景下的 1991—2030 年的日尺度数据。文中采用的 RCP 4.5 情景是在 2100 年左右辐射强迫稳定在 4.5 W/m^2,需要通过能源体系改变、碳捕获等技术的应用对温室气体排放进行限制,较符合我国应对气候变化的政策措施和未来发展愿景。

1.3　GCMs 模式评价方法

本文采用傅国斌等[17]提出的一种评价体系,该体系是将各 GCM 模式数据通过双线性插值到站点和同时期观测值比较,计算出表 1 中的各项评价指标,再采用一个介于 0～9 的秩评分对每一项单独的评价指标进行评分[18],方法为

$$\begin{cases} R_{si}=\dfrac{x_i-x_{\min}}{x_{\max}-x_{\min}}\times 9 \\ R_s=\sum\omega_i R_{si} \end{cases} \tag{1}$$

式中:x_i 为第 i 个评价指标的数值;ω_i 为第 i 个评价指标在秩评分中的权重;R_s 为最终得分,分数越低代表该 GCMs 模式对降水模拟效果越好。

表 1　GCMs 评价指标及权重

评级指标	计算方法	权重
均值	相对误差	1.0
标准差	相对误差	1.0
时间差异	标准化均方根误差(NRMSE)	1.0
年内分布	相关系数	1.0
趋势及其变幅	Mann-Kendall 检验	0.5
	Sen′s 斜率估计	0.5
概率密度函数(PDF)	B_{score}(Brier score)	0.5
	S_{score}(Significance score)	0.5

要计算 GCM 的得分需要分别计算该 GCM 各项评价指标,其中均值、标准差、M-K 趋势统计、Sen′s 斜率定义及计算公式详见文献[19-21]。B_{scorce}反映了模拟值和实测值的概率密度函数之间的均方误差[22-23],其值越小越好,计算公式见式(2);S_{score}计算实测数据和模拟数据的分布在每个等分序列值累计概率的最小值,反映了模拟值和实测值的概率密度函数之间的重叠[24],其计算公式见式(3)。

$$B_{scorce}=\frac{1}{n}\sum_{i=1}^{n}(P_{mi}-P_{oi})^2 \tag{2}$$

$$S_{score}=\sum_{i=1}^{n}\mathrm{Min}(P_{mi},P_{oi}) \tag{3}$$

式中:P_{mi}和 P_{oi}分别为模拟值和实测值 i 等分处的概率密度值;n 为划分的总份数(n=100)。

基于每个模型的评价结果,对模型进行排序,筛选出排名靠前的 6 种气候模式并根据式(4)计算权重,进而构建一个集成气候模式来减少不同模式情景和参数的不确定性。

$$\begin{cases} W_i=R_i/(\sum_{i=1}^{N}R_i) \\ R_i=(\sum_{i=1}^{N}\sqrt{S_i})/\sqrt{S_i} \end{cases} \tag{4}$$

式中:N 为模式个数 ;S_i 为第 i 个模式的评分;W_i 为第 i 个模式的权重。

1.4　统计降尺度模型

SDSM 模型主要内容包括 2 个方面:一是构建

预报量(站点气象要素)与预报因子(大气环流因子)之间的统计关系,从而确定模型;二是根据确定好的模型,利用 GCM 数据驱动生成站点气候要素的未来情景数据[25]。该模型广泛应用于美洲、欧洲、亚洲的气象、水文等领域的研究,其基本原理[26-28]为

$$\omega_i=\alpha_0+\sum_{j=1}^{n}\alpha_j P_{ij};R_i^{0.25}=\beta_0+\sum_{j=1}^{n}\beta_j P_{ij}+e_i \quad (5)$$

$$T_i=\gamma_0+\sum_{j=1}^{n}\gamma_j P_{ij}+e_i \quad (6)$$

式中:P_{ij} 为第 i 天第 j 个预报因子;ω_i 是第 i 天发生降水的概率;α、β、γ 为模式的参数;R_i 为降水量;T_i 为温度变量;e_i 为误差。

2　结果与分析

2.1　CMIP5 多模式对降水模拟能力评估

表 2 列出了各 GCM 和实测值的逐月降水的均值、标准差、标准化均方根误差、年内分布、趋势及其变幅指标、概率密度函数指标及其各 GCM 的综合模拟得分。

固原站多年平均降水量为 436.37 mm,而 GCMs 的模拟降水量的变化范围为 377～716 mm,最大降水量为实测值的 1.5 倍左右。21 个 GCM 模拟降水量的均值和中位值分别是 510.54 mm 和 495.25 mm。相较于实测值 85.9 mm 的标准差,GCM 的模拟的变幅为 48.9～101.66 mm 。相较于实测值,各 GCM 的标准化均方根误差变化范围为 0.57～1.18,标准化均方根误差反映了各 GCM 和实测值之间的偏差,在均值和标准差相同的情况下,GCM 的该值越小则说明模拟性能越优。

各 GCM 的逐月降水量和实测值的相关系数都高于 0.95,说明各 GCM 可以较好地反映降水量的年内变化规律。通过趋势分析,实测降水量呈下降趋势($Z=-0.8$),变幅为 1.01 mm/a。各 GCM 的 Z 值的变化范围为−2.33～1.56,其中有 9 个 GCM 呈下降趋势。

表 2　不同 GCM 下月降水评分

GCM	均值	标准差	NRMSE	年内分布	趋势及变幅		PDF		总评分	排序
					Z	β	B_{score}	S_{score}		
观测值	436.37	85.90			−0.80	−1.01				
ACCESS1.3	377.82	82.57	0.96	0.97	−0.14	−0.41	0.09	81.90	27.94	9
BNU-ESM	396.73	48.90	0.57	0.97	0.57	0.58	0.26	76.76	23.98	5
Bcc-csm1-1-m	496.22	56.77	0.66	0.98	1.59	1.52	0.05	84.91	28.68	10
CanESM2	390.50	61.50	0.72	0.97	0.45	0.45	0.15	80.27	24.40	6
CCSM4	495.25	78.02	0.91	0.96	0.03	0.13	0.02	86.36	27.26	8
CESM1-CAM5	583.05	87.13	1.01	0.97	−0.26	−0.39	0.01	88.00	31.65	16
CSIRO-Mk3-6-0	536.58	61.80	0.72	0.98	1.33	1.47	0.12	80.85	30.30	14
CNRM-CM5	702.98	79.80	0.93	0.99	1.31	1.76	0.13	80.49	39.87	20
GFDL-CM3	485.50	69.93	0.81	0.97	−0.34	−0.26	0.07	83.50	25.29	7
GFDL-ESM2G	592.27	72.31	0.84	0.97	1.31	1.68	0.16	79.96	30.60	15
GFDL-ESM2M	391.45	57.33	0.67	0.98	−2.33	−2.07	0.19	78.96	19.60	2
inmcm4	507.22	91.31	1.06	0.96	0.20	0.17	0.02	86.50	34.79	19
IPSL-CM5A-LR	492.08	70.60	0.82	0.98	−0.80	−1.09	0.12	81.42	29.49	13
IPSL-CM5A-MR	636.70	70.93	0.83	0.99	−1.14	−1.73	0.08	83.04	29.39	12
Miroc5	390.22	64.91	0.76	0.95	−0.88	−0.80	0.17	79.55	18.86	1
MIROC-ESM	449.11	54.38	0.63	0.97	1.05	0.88	0.17	76.57	23.00	3
MIROC-ESM-CHEM	392.82	60.75	0.71	0.97	−0.11	−0.14	0.16	80.26	23.45	4
MPI-ESM-LR	488.45	72.26	0.84	0.97	0.26	0.21	0.21	77.43	29.14	11
MPI-ESM-MR	587.95	83.31	0.97	0.96	1.56	2.07	0.05	84.73	33.60	17
MRI-CGCM3	716.82	101.66	1.18	0.98	−0.23	−0.54	0.01	87.79	43.19	21
NorESM1-M	611.66	67.86	0.79	0.98	0.97	1.10	0.10	82.25	34.23	18

表 2 中概率密度函数的指标反映了 GCM 和实测值在概率上的拟合情况,其中 B_{score} 和 S_{score} 值都是百分比数值。由表 2 可知,所有 GCM 的 B_{score} 指标的变幅为 0.01～0.26,S_{score} 指标的变幅为 76.57～88,CESM1、MRI-CGCM3 和实测值在概率分布上最为拟合,而 Bnu 和 MPI-ESM-LR 在概率分布上

的拟合最差。根据式(1),计算 21 个 GCM 对降水的综合评分,经计算,模拟性能最优的为 Miroc5,模拟性能最差的为 MRI-CGCM3。

依据表 2 评分的排序结果,筛选出排名靠前的 6 种气候模式,分别为:Miroc5、GFDL-ESM2M、MIROC-ESM、MIROC-ESM-CHEM、BNU-ESM 和 CanESM2,通过式(4)计算各气候模式的降水权重,进而生成集成气候模式。

2.2　SDSM 模型率定与验证

基于泾河上游三关口流域 4 个站点 1991—2014 年实测数据,建立预报量降水与所选预报因子 NCEP 的统计降尺度模型,选取 1991—2005 年作为率定期、2006—2014 年作为验证期,将各模式数据通过双线性插值法插值到各站点驱动模型生成模拟值。以泰森多边形法计算各站点面积权重,得到流域上降水量的实测值和模拟值。采用表征回归模型拟合效果的决定系数(R^2)和标准误差(SE)来评价 SDSM 模型在率定期的拟合效果。所得结果显示各模式在率定期中,R^2 在 0.228～0.324,各模式的标准误差 SE 为 0.354～0.450。SDSM 模型也被我国的专家学者应用于很多流域,如郝振纯等[29]、魏凤英等[30],而不同的地区模拟情况有不同的模拟结果,翟文亮等[31]在东江流域模拟降水的 R^2 在 0.23～0.29,刘卫林等[32]在赣江流域模拟降水的 R^2 在 0.20～0.34,比较而言,本文结果较好。这主要与降水变化的复杂性有关,总体上也达到了降水模拟地预期效果。

从图 1 可以看到,在率定期和验证期内泾河上游三关口流域的月均降水量的模拟值与实测值拟合较好,在率定期和验证期两者 Pearson 相关系数分别达到 0.98、0.96,说明 SDSM 模型在泾河上游三关口流域具有较好的适用性,对流域降水的降尺度模拟较为可靠,用于预测泾河上游三关口流域未来降水变化是可行的。

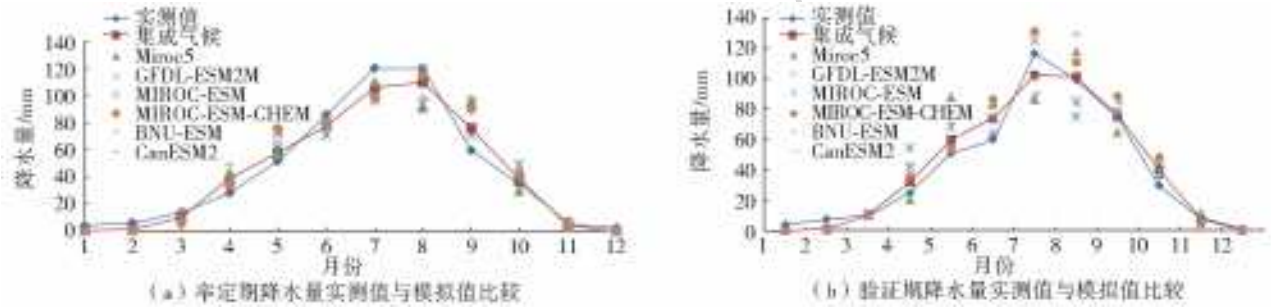

图 1　三关口流域降水量实测值与模拟值比较

图 2 是采用加拿大气象研究中心的气候评价指数[33]对实测数据和降尺度后的 GCMs 输出数据进行计算后绘制的箱型图,用以评价降尺度模型在研究流域的模拟性能。图中 PrcpTot 表示年总降水量;R10 表示年日降水量≥10 mm 的总日数;SDII 表示降水总量和日数的比值;R95pTot 表示日降水>95%分位值的降水量之和。由图 2(a)我们可以看到就 PrcpTot 指标而言,各气候模式的降水经降尺度后较实测值的均值误差在 5%以内,Miroc5 与实测值最为接近。各气候模式的年降水量年际分布各不相同,集成模式因由各模式加权集合得到,其年际差异小且趋近于均值。图 2(b)展示了各气候模式年日降水量≥10 mm 的总日数,可以看到各气候模式均值大都为 13 d 较实测值 15 d 偏少,从侧面可以看出 SDSM 模型降尺度后对极端降水模拟效果不很理想。图 2(c)展示了各气候模式降水总量和日数的比值,其中 GFDL-ESM2M 与实测值更接近。图 2(d)展示了各气候模式日降水>95%分位值的降水量之和,其中 MIROC-ESM-CHEM 与实测值更为接近。综上可知,没有任何一个气候模式优于其他气候模式,而集成气候模式各指标均值与实测值都很接近,表现很好,因此采用集成气候模式能有效减小模拟误差。

2.3　未来降水情景预估

基于构建的统计降尺度模型 SDSM,使用优选的 6 个 GCM 模式模拟生成泾河上游三关口流域基准期和未来的降水数据。以 1991—2014 年的多年年均降水量为基准值,对基准期(1991—2014 年)和未来时期(2015—2030 年)的年降水量进行距平计算,结果见图 3。黑色竖线之前的是基准期的实测值,之后是各 GCM 模式预估的未来年降水量。相较于基准期,不同气候模式所预估的未来降水量存在较大差异性,大部分 GCM 模式较基准期有所增加。MIROC-ESM-CHEM 预估的未来气候多年年均降水量增加的最多,为 55 mm,而 CanESM2 则减少了 22 mm,Miroc5、GFDL-ESM2M、MIROC-ESM、BNU-ESM 分别增加了 20、23、29、46 mm。就集成气候模式而言:2015—2030 年期间,集成模式年降水量在正距

平和负距平状态之间波动,但大多数为正距平,其多年均值较基准期增加了 26 mm(4.8%),且以 9 mm/(10 a)的速度增长。多模式集合使得其在降水量极值上受到削减,但更能反映整体的趋势。

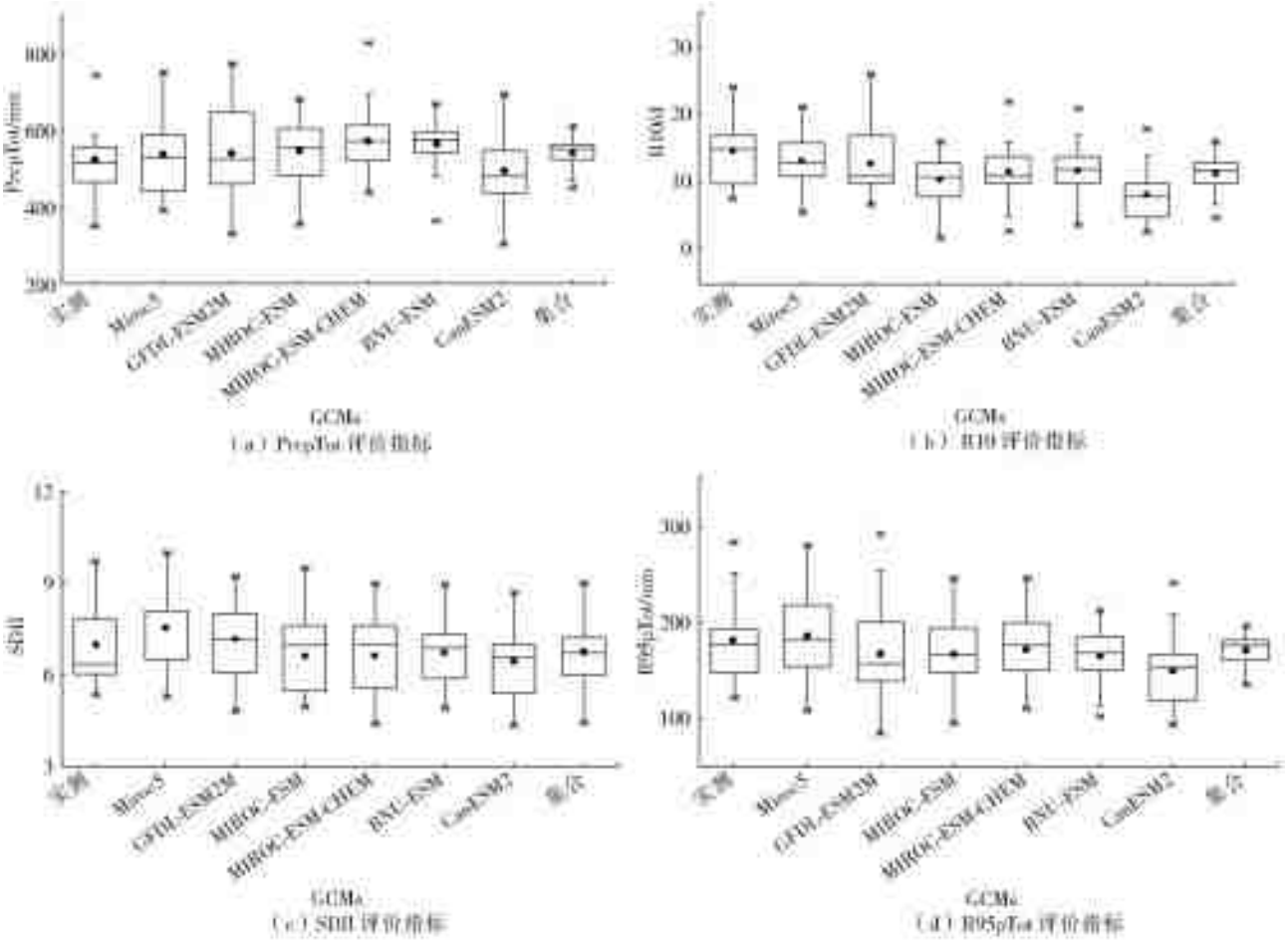

图 2　降水降尺度各评价指标箱型图

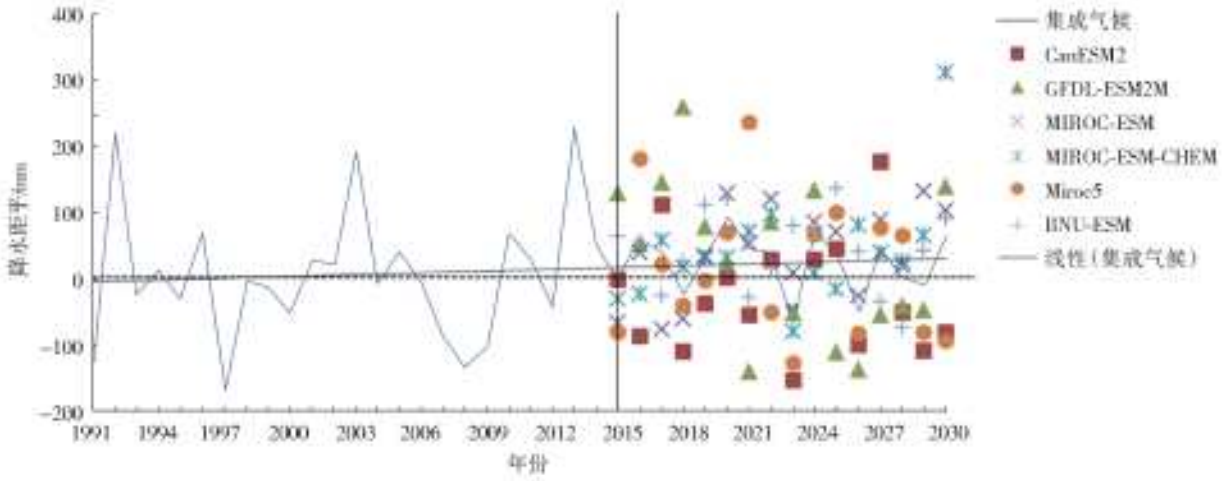

图 3　多模式下流域降水变化的情景预估

图 4 所示为 6 种气候模式和集成模式所预估的未来时期降水的年内分布,作为对比,图 4 同时还列出了基准期的年内分布情况。未来时期的 3—6 月份的降水量较基准期增加,7、9 月降水量呈下降趋势,8 月降水量变化不大。不同的气候模式预估的降水量具有一定的不确定性,例如 GFDL-ESM2M 预估的 7 月降水量只有 78 mm,而 MIROC-ESM-CHEM 预估的 10 月降水量有 65 mm 之多。就集成气候模式而言,与基准期相比,其春季降水增多,夏季降水减少。

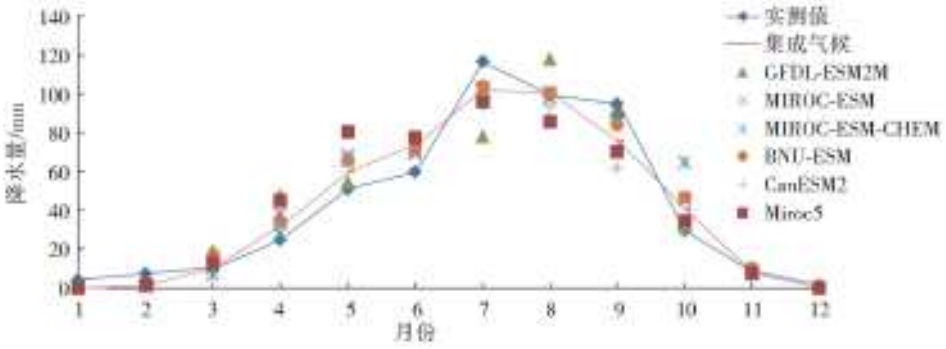

图 4　未来时期的降水年内分布

3　结　论

(1)通过多模式秩评分法可知 Miroc5、GFDL-ESM2M、MIROC-ESM、MIROC-ESM-CHEM、BNU-ESM 和 CanESM2 较其他气候模式更为适合泾河上游三关口流域的气候变量模拟。

(2)统计降尺度模型 SDSM 在泾河上游三关口流域取得较好模拟效果:各模式在率定期中的 R^2 在 0.228～0.324,标准误差在 0.354～0.450;在率定期和验证期内,实测值与模拟值年内分布接近;各模式在气候评价指标上各有优劣,集成模式在各项指标上都较为接近实测值,总体来说降尺度结果较为可靠。

(3)较 1991—2014 年,各模式泾河上游三关口流域多年年均降水量有增有减,大部分呈增长趋势且集成气候模式较历史时期增长了 26 mm(4.8%)。泾河上游三关口流域未来降水量随季节变化明显,呈现春季降水增多、夏季降水减少的现象。

本文在气候变化对流域降水预估过程中的 GCMs模式的不确定性、降尺度方法的不确定性都会导致最终结果存在不确定性。本文采用多模式集合就是为了在保持气候模式自身特性的前提下,在一定程度上削弱气候模式之间的不确定性。但本文仅采用了一种降尺度方法,在以后的研究中可以增加更多的评价指标,采用更多的降尺度方法进行对比,综合分析未来气候变化,减少模拟结果的不确定性。

参考文献:

[1] 曹颖,张光辉,罗榕婷. 全球气候变化对泾河流域径流和输沙量的潜在影响[J]. 中国水土保持科学,2010,8(2):30-35. DOI:10.16843/j.sswc.2010.02.006.

[2] ZHOU T J. A robustness analysis of CMIP5 models over the east Asia-western north Pacific domain[J]. Engineering, 2017, 773-778. DOI: 10.1016/J.ENG.2017.05.018.

[3] ARNELL N W. Climate change and global water resources[J]. Global Environmental Change, 1999, 9(SI):31-49.

[4] VARIS O,KAJANDER T,LEMMELA R. Climate and water:from climate models to water resources management and vice versa[J]. Climate Change,2004 ,66(3):321-344.

[5] 刘昌明,刘文彬,傅国斌,等. 气候影响评价中统计降尺度若干问题的探讨[J]. 水科学进展,2012,23(3):427-437. DOI:10.14042/j.cnki.32.1309.2012.03.016.

[6] ROSANA N F,MARK R N,THOMAS M R. Climate change effects on summertime precipitation organization in the southeast United States[J]. Atmospheric Research, 2018(214): 348-363. DOI: 10.1016/j.atmosres.2018.08.012.

[7] LU G,JIE H,XINGWEI C,et al. Contributions of natural climate changes and human activities to the trend of extreme precipitation[J]. Atmospheric Research, 2018(205):60-69. DOI:10.1016/j.atmosres.2018.02.006.

[8] MEARNS L,BOGARDI I,GIORGI F,et al. Comparison of climate change scenarios generated from regional climate model experiments and statistical downscaling[J]. Journal of Geophysical Research-Atmospheres, 1999,104(D6):6603-6621.

[9] 杨肖丽,郑巍斐,林长清,等. 基于统计降尺度和 SPI 的黄河流域干旱预测[J]. 河海大学学报(自然科学版),2017,45(5):377-383. DOI:10.3876/j.issn.1000-1980.2017.05.001.

[10] HASAN D S,RATNAYAKE U,SHAMS S,et al. Prediction of climate change in Brunei Darussalam using statistical downscaling model[J]. Theoretical & Applied Climatology,2018,133(1-2):343-360. DOI:10.1007/s00704-017-2172-z.

[11] HUANG J,ZHANG J C,ZHANG Z X,et al. Estimation of future precipitation change in the Yangtze River basin by using statistical downscaling method[J]. Stochastic Environmental Research and Risk Assessment,2011,25(6):781-792.

[12] LIU N,LI S L. Predicting summer rainfall over the Yangtze-Huai region based on time-scale decomposition statistical downscaling[J]. Weather and Forecasting,2014,29(1):162-176. DOI:10.1175/WAF-D-13-00045.1

[13] 陈鹏翔,江志红,彭冬梅. 基于 BP-CCA 统计降尺度的中亚春季降水的多模式集合模拟与预估[J]. 气象学报,2017,75(2):236-247. DOI:10.11676/qxxb2017.017.

[14] 李巧玲,王荣克,董小涛. 泾河上游植被覆盖动态及其与降水径流的关系[J]. 水力发电,2015,41(11):21-33. DOI:10.3969/j.issn.0559-9342.2015.11.006.

[15] DUFRESNE J L,FOUJOLS M A,DENVIL S,et al. Climate change projections using the IPSL-CM5 earth system model: from CMIP3 to CMIP5[J]. Climate Dynamics,2013,40(9/10):2123-2165. DOI:10.1007/s00382-012-1636-1.

[16] SPERBER K R,ANNAMALAI H,KANG I S,et al. The Asian summer monsoon: an intercomparison of CMIP5 vs. CMIP3 simulations of the late 20th century[J]. Climate Dynamics,2013,41(9/10):2711-2744. DOI:10.1007/s00382-012-1607-6.

[17] FU G B,LIU Z F,CHARLES S P,et al. A score-based method for assessing the performance of GCMs:A case study of southeastern Australia[J]. Journal of Geophysical Research Atmospheres,2013,118(10):4154-4167. DOI:10.1002/jgrd.50269.

[18] 陈思淳,黄本胜,王晓刚,等. 杨楼流域降水变化特征及 CMIP5 气候模式评估[J]. 人民珠江,2018,39(6):58-62,97. DOI:10.3969/j.issn.1001-9235.2018.06.013.

[19] SEO K H,OK J. Assessing future changes in the east Asian summer monsoon using CMIP3 models:results from the best model ensemble[J]. Journal of Climate,2013,26(19):7662-7675.

[20] MANN H B. Nonparametric test against trend[J]. Econometrica,1945,13(3):245-259.

[21] KAHYA E,KALAYC S. Trend analysis of streamflow in Turkey[J]. Journal of Hydrology,2004,289(1-4):128-144.

[22] FERRO C A,FRICKER T E. A bias-corrected decomposition of the brier score[J]. Quarterly Journal of Royal Meteorological Society,2012,138(668):1954-1960.

[23] KNUTSON T R,DELWORTH T L,DIXON K W,et al. Model assessment of regional surface temperature trends(1949-1997)[J]. Journal of Geophysical Research ,1999,104(24):30981-30996.

[24] HAY L E,WILBY R L,LEAVESLEY G H. A comparison of delta change and downscaled GCM scenarios for three mountaidous basins in the Unted States[J]. Jawra Journal of the Americsn Water Resources Association,2000,36(2):387-397.

[25] WILLBY R L,DAWSON C W,BARROW E M. SDSM 4.2:A decision support tool for the assessment of regional climate change impacts[J]. Environmental Modelling & Software,2007,145-157.

[26] MOHSEN A,HUSEYIN T. Future changes in maximum temperature using the statistical downscaling model (SDSM) at selected stations of Iran[J]. Modeling Earth Systems and Environment, 2016, 2(2):2363-6203. DOI:10.1007/s40808-016-0112-z.

[27] ZULKARNAIN H,SUPIAH S,SOBRI H. Application of SDSM and LARS-WG for simulating and downscaling of rainfall and temperature[J]. Theoretical and Applied Climatology, 2014, 116(1-2):243-257. DOI:10.1007/s00704-013-0951-8.

[28] 代慧慧,杨汉波,胡庆芳. 基于 SDSM 的疏勒河流域气候变化统计降尺度研究[J]. 水利水运工程学报,2015(5):46-53. DOI:10.16198/j.cnki.1009-640X.2015.05.006.

[29] 郝振纯,时芳欣,王加虎. 统计降尺度法在黄河源区未来降水变化分析中的应用[J]. 水电能源科学,2011(3):1-4.

[30] 魏凤英,黄嘉佑. 我国东部夏季降水量统计降尺度的可预测性研究[J]. 热带气象学报,2010,26(4):483-490.

[31] 翟文亮,李朋俊,林凯荣. 基于 SDSM-SWAT 的气候变化下东江流域径流预测模拟[J]. 人民珠江,2016,37(4):1-6. DOI:10.3969/j.issn.1001-9235.2016.04.001

[32] 刘卫林,熊翰林,刘丽娜. 基于 CMIP5 模式和 SDSM 的赣江流域未来气候变化情景预估[J]. 水土保持研究,2019,26(2):145-152. DOI:10.13869/j.cnki.rswc.2019.02.021.

[33] LI W,JIANG Z H,XU J J. Extreme precipitation indices over China in CMIP5 models. Part II:probabilistic projection[J]. Journal of Climate,2016,29(24):8989-9004. DOI:10.1175/JCLI-D-16-0377.1.

·译文(Translation)·

DOI:10.13476/j.cnki.nsbdqk.2020.0111

Projection of future precipitation changes in upper Jinghe River basin using multiple models

LOU Wei, LI Zhijia, LIU Yuhuan

(College of Hydrology and Water Resources, Hohai University, Nanjing 210098, China)

Abstract: The prediction of precipitation changes in the future can provide a basis for research on water resource changes in the upper Jinghe River basin. The GCMs are ranked according to the site measured data and monthly GCMs data. The statistical downscaling model SDSM is constructed based on daily data of 6 GCM models selected from 21 GCMs, the climate models integrated by 6 GCMs, in situ stations data, and NCEP reanalysis data, to predict the future precipitation change in the upper reaches of Jinghe River. The results show that the SDSM is reliable for precipitation simulation. The R^2 of each model is between 0.228 and 0.324 , the standard error is between 0.354 and 0.450, respectively. The simulated monthly average precipitation in the periodic and verification periods is similar to the measured value and the distribution is similar within a year. The integrated model performs best in the downscaling performance evaluation period. Under the RCP 4.5 scenario, most future precipitation models and integrated models in the upper Jinghe River show an increasing trend. By the 2030s, precipitation in the upper Jinghe River may increase by 4.8%, and local rainfall in spring also exhibits an increasing trend, and summer rainfall may decrease.

Key words: climate change; precipitation; rank score evaluation; SDSM; upper Jinghe River basin

Jinghe River, the secondary tributary and one of the top ten river systems of the Yellow River, has an average annual precipitation of 350-600 mm and belongs to the semi-humid and semi-arid transition region[1]. The Sanguankou watershed of the upper reaches of the Jinghe River is located in the Ningnan Mountains in the west of the Loess Plateau. Due to the impact of climate change, local soil erosion and water shortage are becoming increasingly prominent, which has become the bottleneck hindering the local economic development. Therefore, it is of great necessity to qualitatively and quantitatively study the impact of future climate change on water resources in the upper Jinghe River region.

At present, a common way to study the future climate change of a region is to use the output data of global climate models (GCMs) combined with different downscaling methods to predict the future climate change scenarios of a region. GCM can better simulate the most important average characteristics of large-scale climate information, so this method has been widely used in the research on the impact of climate change on hydrology and water resources[2-7]. The downscaling methods can be divided into three categories: statistical downscaling model(SDSM), dynamic downscaling, and the combination of statistical downscaling and dynamic

Received: 2020-02-19 **Revised**: 2020-06-03 **Online publishing**: 2020-06-23
Online publishing address: https://kns.cnki.net/kcms/detail/13.1430.TV.20200623.0928.004.html
Funds: National Natural Science Foundation of China(51679061); Key Research and Development Program of Ningxia Autonomous Region (2018BEG02010)
Author brief: LOU Wei (1996-), male, Anqing, Anhui Province, mainly engaged in hydrometeorology and hydrology forecast. E-mail: 18856329193@163.com
Corresponding author: LI Zhijia(1962-), male, professor, PhD, Yuncheng, Shanxi Province, mainly engaged in simulation and prediction of hydrophysical laws. E-mail: zjli@hhu.edu.cn

downscaling. Each method has its own advantages and disadvantages. For example, SDSM has the advantages including small calculation amount and easy construction of the model, without considering the impact of boundary conditions on the prediction results, which has been favored in climate change studies[8-9]. Scholars have made great achievements in the prediction of temperature and precipitation by using GCM combined with SDSM. For example: Hasan et al. [10] utilized SDSM combined with GCM to predict the maximum temperature, minimum temperature, and precipitation in Brunei from 2017 to 2076, finding that the maximum temperature showed an increasing trend while the minimum temperature and precipitation exhibited a decreasing trend. Huang et al. [11] and Liu et al. [12] predicted the future precipitation in the Yangtze River basin and the middle and lower reaches of the Yangtze River respectively via SDSM, and the results showed that most areas in the Yangtze River basin would be dominated by an upward trend. Chen et al. [13] estimated the precipitation in spring in central Asia based on the multi-model set of statistical downscaling, finding that the multi-model set was superior to most of the single-model downscaling results.

In this paper, a rank score method based on multi-objective function is adopted to evaluate the monthly precipitation output data of 21 GCMs provided by CMIP5, and 6 GCMs are selected. SDSM model is driven by 6 kinds of GCM daily precipitation data to generate the future climate change scenario of the upper Jinghe River basin, which cannot only solve the adaptability problem of different GCM regions and reduce the uncertainty of single GCM simulation, but also provide the climate change range in multiple models and multi-model set, so as to provide the basis for local governments to work out more effective water use plans and better tap the potential of water resources.

1 Research method

1.1 Overview of the research area

The upstream basin of Jinghe River in this paper refers to the controlled basin above the Sanguankou hydrological station located in the east side of Liupan Mountain within Jingyuan county, Ningxia province. There are Dawan, Wating, Shizi and other precipitation stations in the basin, and Guyuan weather station with rich historical meteorological data is set near the basin. The basin covers an area of 218 km^2, and the precipitation mainly concentrates from June to September[14]. The basin is located at the eastern foot of Liupan Mountain, with an altitude of from 1,640 m to 2,930 m. It belongs to the rocky and forest region, which is affected by the southeast monsoon in summer and controlled by the Mongolian high pressure in winter with significant continental monsoon climate and alpine mountain climate characteristics.

1.2 Data resources

This study requires three types of data: precipitation data measured at the station, the U S National Centers for Environmental Prediction (NCEP) reanalysis data, and output data of current and future climatic conditions simulated by GCM. The precipitation data measured at the station can be obtained by reference to relevant hydrological yearbooks, and the daily precipitation data of Dawan, Wating, Shizi, and Sanguankou in the upstream of Jinghe River basin from 1991 to 2014 can be obtained. The monthly precipitation data of Guyuan station near the river basin from 1970 to 2005 are obtained from website of China meteorological data(http://data.cma.cn/) for the evaluation of GCMs to select 6 GCMs closer to the local location. Among them, the data accuracy of precipitation data obtained from hydrological yearbook and http://data.cma.cn/ is 0.1 mm, so they are put together for use. NCEP reanalysis data are jointly provided by the NCEP and the National Center for Atmospheric Research (NCAR). The time selected period coincides with the measured data(from 1991 to 2014), including the meteorological data such as precipitation, average surface temperature, specific humidity, relative humidity, u and v components of wind speed. GCM data are downloaded from CMIP5(https://esgf-node.llnl.gov/projects/cmip5/). Compared with the previous models, CMIP5 adopts a more reasonable parame-

terization, flux treatment scheme, and the coupler technology to get more accurate and detailed data[15,16]. The monthly precipitation outputs from 1970 to 2005 of 21 GCM models in the RCP 4.5 scenario and the daily scale data from 1991 to 2030 of the selected 6 GCM models in the RCP 4.5 scenario are downloaded. The scenario of RCP 4.5 adopted in this paper is that the radiation is forced to stabilize at 4.5 W/m^2 around the year of 2100, and the greenhouse gas emissions need to be limited through the change of energy system and the application of carbon capture technology, which is more in line with China's policies and measures to deal with climate change and future development vision.

1.3 GCMs model evaluation method

In this paper, an evaluation system proposed by Fu Guobin et al.[17] is adopted. In this system, all evaluation indexes in Tab. 1 are calculated by comparing the data of each GCM to the station and the measured values in the same period through bilinear interpolation. Then, a rank score between 0 and 9 is adopted to score each individual evaluation index[18], as shown in Eq. (1)

$$\begin{cases} R_{si}=\dfrac{x_i-x_{\min}}{x_{\max}-x_{\min}}\times 9 \\ R_s=\sum \omega_i R_{si} \end{cases} \tag{1}$$

where: x_i is the numerical value of the ith evaluation index; ω_i is the weight of the ith evaluation index in the rank score; R_s is the final score, the lower the score is, the better the simulation effect of the GCMs on precipitation is.

Tab. 1 GCMs evaluation indicators and weights

Evaluation indexes	Calculation methods	Weights
Mean value	Relative error	1.0
Standard deviation	Relative error	1.0
Time difference	Normalized root-mean-square error	1.0
Annual distribution	Correlation coefficient	1.0
Trends and their variations	Mann-Kendall test	0.5
	Sen's slope estimate	0.5
Probability density function(PDF)	Brier score (B_{score})	0.5
	Significance score(S_{score})	0.5

Each evaluation index of the GCM should be calculated separately, including mean value, standard deviation, M-K trend statistics, definition of Sen's slope and calculation formula to calculate the score of GCM, see References [19-21] for details. B_{score} reflects the mean square error between the probability density function of the simulated value and the measured value[22-23], which can be calculated by Eq. (2). A lower value means a better result. S_{score} calculates the minimum cumulative probability of the distribution of measured data and simulated data in each equipartition sequence value, which reflects the overlap between the probability density function of simulated value and measured value[24], and its calculation formula is shown in Eq. (3)

$$B_{score}=\frac{1}{n}\sum_{i=1}^{n}(P_{mi}-P_{oi})^2 \tag{2}$$

$$S_{score}=\sum_{i=1}^{n}\mathrm{Min}(P_{mi},P_{oi}) \tag{3}$$

where: P_{mi} and P_{oi} are the probability density values of simulated value and measured value i respectively; n is the total number of shares divided ($n=100$).

Based on the evaluation results of each model, the models are ranked. The top six climate models are selected and the weights are calculated according to Eq. (4) to construct an integrated climate model so as to reduce the uncertainty of scenarios and parameters of different models

$$\begin{cases} W_i=R_i/(\sum_{i=1}^{N}R_i) \\ R_i=(\sum_{i=1}^{N}\sqrt{S_i})/\sqrt{S_i} \end{cases} \tag{4}$$

where: N is the number of models; S_i is the score of the ith model; W_i is the weight of the ith model.

1.4 Statistical downscaling model

SDSM mainly includes two aspects: one is to establish the statistical relationship between the forecast quantity (meteorological elements of the site) and the forecast factor (atmospheric circulation factor), so as to determine the model; the other is that according to the determined model, the future scenario data of the site climate elements can be generated with GCM data[25]. This model is widely used in the study of meteorology, hydrology, and other fields in America, Europe and Asia, and its basic principle[26-28] is as follows

$$\omega_i=\alpha_0+\sum_{j=1}^{n}\alpha_j P_{ij};R_i^{0.25}=\beta_0+\sum_{j=1}^{n}\beta_j P_{ij}+e_i \tag{5}$$

$$T_i = \gamma_0 + \sum_{j=1}^{n} \gamma_j P_{ij} + e_i \quad (6)$$

where: P_{ij} is the j th predictor on day i; ω_i is the probability of precipitation occurring on the ith day; α, β, and γ are the parameters of the model; R_i is the precipitation; T_i is the temperature variable; e_i is the error.

2 Results and analysis

2.1 CMIP5 multi-model assessment of precipitation simulation capability

Tab. 2 lists the mean value, standard deviation, normalized root-mean-square error, annual distribution, trend and variation indicators, probability density function indicators of each GCM and measured monthly precipitation, as well as the comprehensive simulation score of each GCM.

The average annual precipitation of Guyuan station is 436.37 mm, while the range of simulated precipitation of GCMs is 377-716 mm, and the maximum precipitation is about 1.5 times of the measured value. The mean and median values of the 21 GCM simulated precipitation are 510.54 mm and 495.25 mm, respectively. Compared with the standard deviation of the measured value of 85.9 mm, the simulated amplitude of GCM is 48.9-101.66 mm while compared with that of the measured values, the normalized root-mean-square errors of each GCM range from 0.57 to 1.18. The normalized root-mean-square error reflects the deviation between each GCM and the measured value. Under the same mean value and standard deviation, a lower GCM value suggests better simulation performance.

The correlation coefficient between monthly precipitation and measured values of each GCM is higher than 0.95, indicating that each GCM can well reflect the annual change rule of precipitation. According to the trend analysis, the measured precipitation shows a downward trend ($Z = -0.8$), with a variation of 1.01 mm/a. The Z value of each GCM varies from -2.33 to 1.56, among which nine GCMs show a downward trend.

The indicators of the probability density function in Tab. 2 reflect the fitting of GCM and measured values in probability, where B_{score} and S_{score} values are both percentage values. As can be seen from Tab. 2, the variation of B_{score} indicators of all GCM ranges from 0.01 to 0.26, and the variation of S_{score} indicators ranges from 76.57 to 88. CESM1, MMR-CGCM3 and measured values are the most fitting in the probability distribution, while Bnu and MPI-ESM-LR are the worst. According to Eq. (1), the comprehensive scores of 21 GCMs on precipitation are calculated. After calculation, Miroc5 is the one with the best simulation performance, and MRI-CGCM3 is the one with the worst simulation performance.

According to the ranking results in Tab. 2, the top six climate models are selected, namely Miroc5, GFDL-ESM2M, MIROC-ESM, MIROC-ESM-CHEM, BNU-ESM, and CanESM2. The precipitation weight of each climate model is calculated by Eq. (4) to generate the integrated climate model.

2.2 Calibration and validation of SDSM

Based on the measured data of four stations in Sanguankou watershed of the upstream of Jinghe River from 1991 to 2014, a SDSM of the forecast rainfall and the selected forecast factor NCEP is established. The period from 1991 to 2005 is selected as the calibration period, and the period from 2006 to 2014 is selected as the verification period. The model data are interpolated into the driving model of each station by bilinear interpolation to generate simulation values. The area weight of each station is calculated by Thiessen Polygons method, and the measured and simulated values of precipitation in the basin are obtained. The determination coefficient(R^2) and standard error(SE) representing the fitting effect of regression model are used to evaluate the fitting effect of SDSM in the calibration period, showing that R^2 ranges from 0.228 to 0.324 and the SE of each model is from 0.354 to 0.450. SDSM model is also adopted by experts and scholars including Hao et al.[29] and Wei et al.[30] in many basins in our country, and different areas have varying simulation results under different simulations conditions. For example, the precipitation R^2 simulated by Zhai et al.[31] in the Dongjiang River watershed ranges from 0.23 to 0.29 while

the precipitation R^2 simulated by Liu et al.[32] in the Ganjiang River watershed ranges from 0.20 to 0.34. In comparison, the present results in this paper are better. Since it is mainly related to the complexity of precipitation change, it achieves the expected effect of precipitation simulation in general as well.

Tab. 2 Monthly precipitation score table of different GCMs

GCM	Mean value	Standard deviation	NRMSE	Annual distribution	Trends and variations		PDF		Total score	Rank
					Z	β	B_{score}	S_{score}		
Measured value	436.37	85.90			−0.80	−1.01				
ACCESS1.3	377.82	82.57	0.96	0.97	−0.14	−0.41	0.09	81.90	27.94	9
BNU-ESM	396.73	48.90	0.57	0.97	0.57	0.58	0.26	76.76	23.98	5
Bcc-csm1-1-m	496.22	56.77	0.66	0.98	1.59	1.52	0.05	84.91	28.68	10
CanESM2	390.50	61.50	0.72	0.97	0.45	0.45	0.15	80.27	24.40	6
CCSM4	495.25	78.02	0.91	0.96	0.03	0.13	0.02	86.36	27.26	8
CESM1-CAM5	583.05	87.13	1.01	0.97	−0.26	−0.39	0.01	88.00	31.65	16
CSIRO-Mk3-6-0	536.58	61.80	0.72	0.98	1.33	1.47	0.12	80.85	30.30	14
CNRM-CM5	702.98	79.80	0.93	0.99	1.31	1.76	0.13	80.49	39.87	20
GFDL-CM3	485.50	69.93	0.81	0.97	−0.34	−0.26	0.07	83.50	25.29	7
GFDL-ESM2G	592.27	72.31	0.84	0.97	1.31	1.68	0.16	79.96	30.60	15
GFDL-ESM2M	391.45	57.33	0.67	0.98	−2.33	−2.07	0.19	78.96	19.60	2
inmcm4	507.22	91.31	1.06	0.96	0.20	0.17	0.02	86.50	34.79	19
IPSL-CM5A-LR	492.08	70.60	0.82	0.98	−0.80	−1.09	0.12	81.42	29.49	13
IPSL-CM5A-MR	636.70	70.93	0.83	0.99	−1.14	−1.73	0.08	83.04	29.39	12
Miroc5	390.22	64.91	0.76	0.95	−0.88	−0.80	0.17	79.55	18.86	1
MIROC-ESM	449.11	54.38	0.63	0.97	1.05	0.88	0.17	76.57	23.00	3
MIROC-ESM-CHEM	392.82	60.75	0.71	0.97	−0.11	−0.14	0.16	80.26	23.45	4
MPI-ESM-LR	488.45	72.26	0.84	0.97	0.26	0.21	0.21	77.43	29.14	11
MPI-ESM-MR	587.95	83.31	0.97	0.96	1.56	2.07	0.05	84.73	33.60	17
MRI-CGCM3	716.82	101.66	1.18	0.98	−0.23	−0.54	0.01	87.79	43.19	21
NorESM1-M	611.66	67.86	0.79	0.98	0.97	1.10	0.10	82.25	34.23	18

In Fig. 1, the simulated monthly average precipitations of Sanguankou watershed on the upper reaches of the Jinghe River during the calibration and validation periods are well fitted to the measured values and the Pearson correlation coefficient reaches 0.98 and 0.96 respectively, indicating that SDSM has a good applicability in Sanguankou watershed of the upstream of Jinghe River, and the downscaling simulation of the precipitation in the watershed is more reliable, so it is feasible to predict the future precipitation changes in Sanguankou watershed of the upstream of Jinghe River.

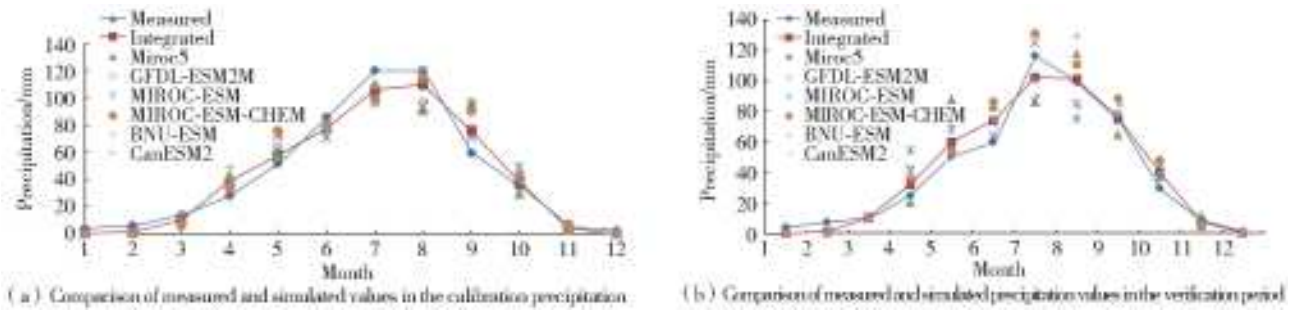

Fig. 1 Comparison of measured and simulated precipitation in Sanguankou watershed

Fig. 2 is the box chart which is drawn with the measured data and the output data of the GCMs calculated after the downscaling, based on the climate evaluation index[33] of the Canadian Meteoro-

logical Research Center, so as to evaluate the simulation performance of the downscaling model in the study watershed. In the figure, PrcpTot represents the total annual precipitation; R10 represents the total number of days with annual daily precipitation≥10 mm; SDII represents the ratio of total precipitation to the number of days; R95pTot represents the total amount of precipitation of >95th percentile of daily precipitation. It can be seen from Fig. 2(a) that, as far as PrcpTot index is concerned, the mean error of precipitation in each climate model compared with the measured value is within 5% after downscaling, and Miroc5 is the closest to the measured value. The inter-annual distribution of annual precipitation of each climate model varies, and the integrated model is obtained by the weighted aggregation of each model. The inter-annual difference is small and close to the mean value. Fig. 2(b) shows the total number of days with annual daily precipitation≥10 mm in each climate model, and thus it can be found that the average value of each climate model is 13 days, lower than the measured value of 15 days. It can be seen from the side that SDSM is not very ideal for extreme precipitation simulation after downscaling. In Fig. 2(c), it shows the ratio of total precipitation and number of days in each climate model, in which the GFDL-ESM2M is closer to the measured value. Fig. 2(d) shows the sum of the precipitation of >95th percentile of daily precipitation for each climate model, in which MIROC- ESM-CHEM is the closest to the measured value. In conclusion, none of the climate models is better than other climate models, while the average value of all indexes of the integrated climate model is close to the measured value, signaling satisfying performance. Therefore, the adoption of the integrated climate model can effectively reduce the simulation error.

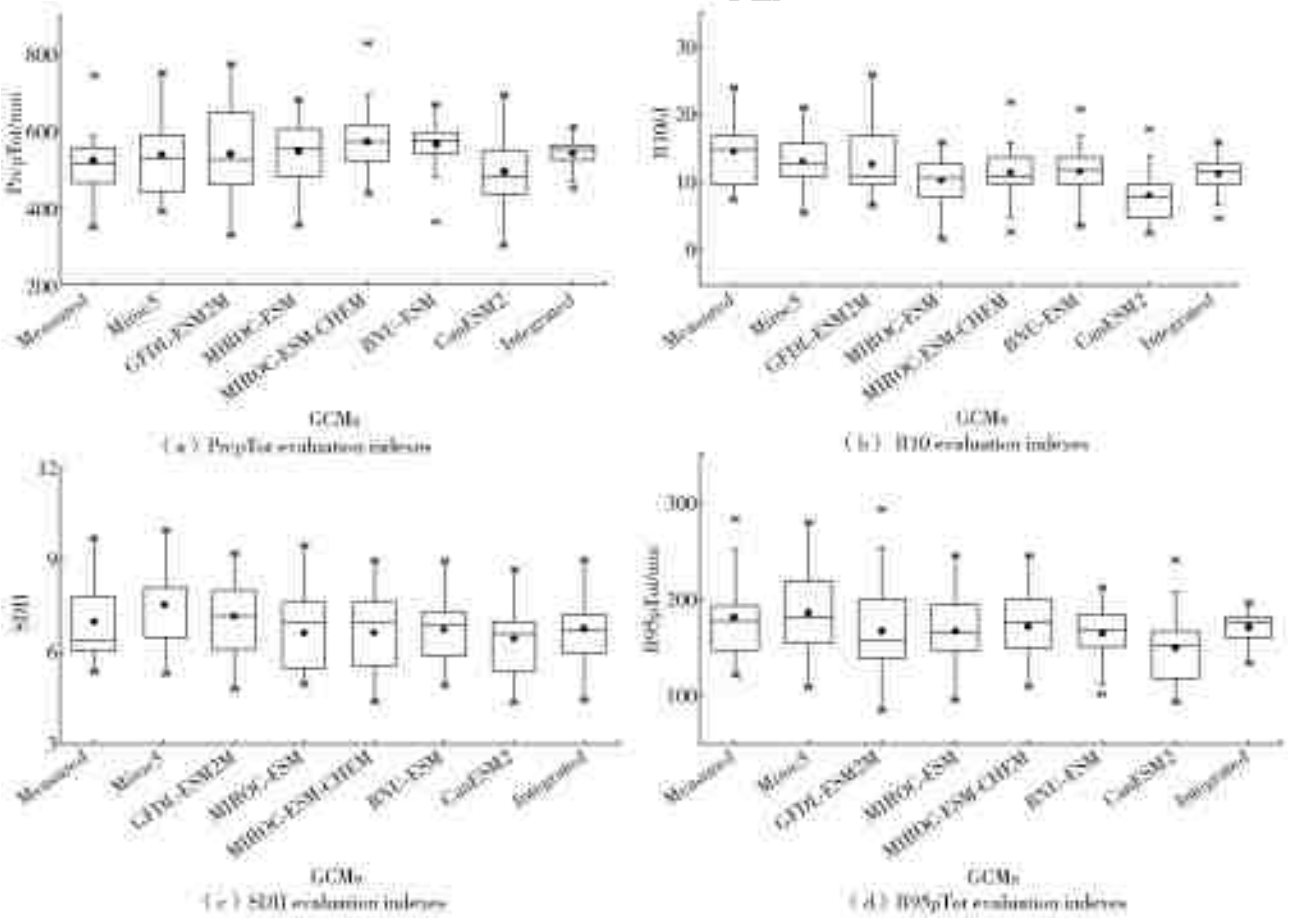

Fig. 2 Box chart for each precipitation downscaling evaluation index

2.3 Forecast of future precipitation scenarios

Based on the established SDSM, the selected six GCM models are used to simulate and generate the baseline period and future precipitation data of Sanguankou watershed in the upstream of Jinghe River. The annual average annual precipitation of

1991-2014 is taken as the base value to calculate the annual precipitation anomaly of the base period (1991-2014) and the future period (2015-2030). The results are shown in Fig. 3. The black vertical bar is preceded by the measured values of the base period, followed by the estimated future annual precipitation of each GCM. Compared with the base period, the future precipitations estimated by different climate models have huge differences, and most GCMs have increased compared with the base period. MIROC-ESM-CHEM forecast for future climate shows the greatest increase by 55 mm in multi-year annual precipitation, while CanESM2 is reduced by 22 mm, and Miroc5, GFDL-ESM2M, MiROC-ESM, and BNU-ESM are raised by 20, 23, 29, and 46 mm, respectively. As for the integrated climate model, from 2015 to 2030, the annual precipitation of the integrated model fluctuates between positive anomaly and negative anomaly, but most of them are positive anomaly, with an annual mean increase of 26 mm(4.8%) compared with the base period and an increase rate of 9 mm/(10 a). Because of the multi-model set, the precipitation extreme value is reduced, but it can better reflect the overall trend.

Fig. 4 shows the annual precipitation distribution predicted by the six climate models and the integrated model in the future period. For comparison, the annual precipitation distribution in the base period is also presented. In the future period, the precipitation from March to June will increase compared with the base period, and the precipitations in July and September show the downward trend, while the precipitation in August sees little change. Different climate models forecast precipitation with some uncertainty. For example, GFDL-ESM2M estimates only 78 mm of precipitation in July, while MIROC ESM-Chem estimates 65 mm of precipitation in October. As for the integrated climate model, compared with the base period, the precipitation in spring increases and the precipitation in summer decreases.

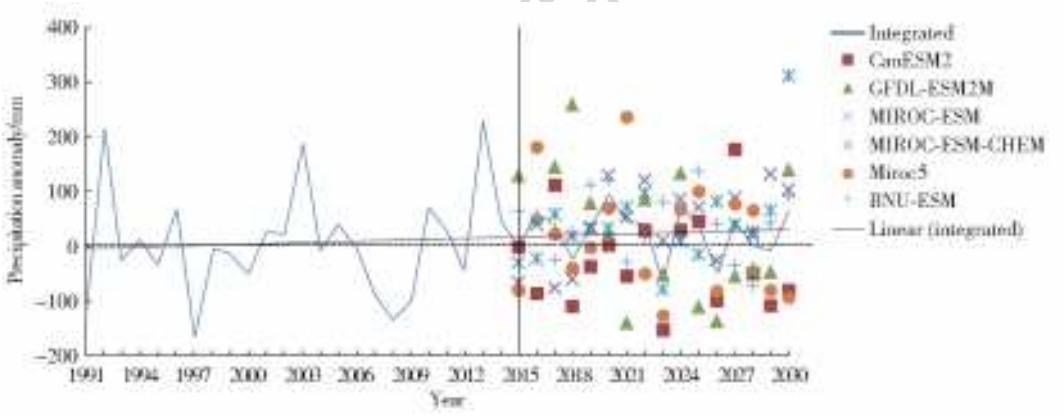

Fig. 3 Scenario estimation of precipitation change under multi-model in the watershed

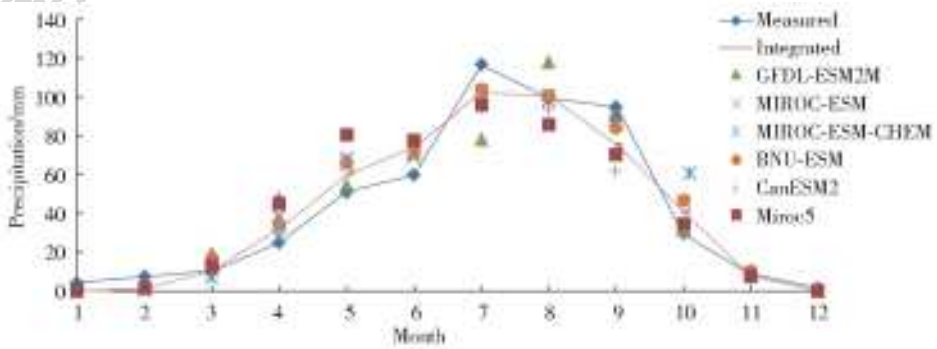

Fig. 4 Annual precipitation distribution in future period

3 Conclusions

(1) Compared with other climate models, Miroc5, GFDL-ESM2M, MIROC-ESM, MiROC-ESM-Chem, BNU-ESM, and CanESM2 are more suitable for the simulation of climate variables in Sanguankou

watershed of the upper Jinghe River with the multi-model rank score method.

(2) SDSM achieves good simulation effect in Sanguankou watershed of the upper Jinghe River. The R^2 of each model in the calibration period is 0.228-0.324, and the SE is 0.354-0.450. The distributions of measured and simulated values are close to each other during the calibration and validation period. Each model has its own advantages and disadvantages in terms of climate evaluation indexes, and the integrated model is close to the measured values in terms of all indexes. In general, the downscaling results can be considered reliable.

(3) Compared with those during 1991 to 2014, the annual average precipitation of Sanguankou watershed of the upper Jinghe River in each model increases or decreases, most of which shows an increasing trend, and the integrated climate model increased by 26 mm(4.8%) compared with the historical period. The future precipitation of Sanguankou watershed of the upper Jinghe River varies significantly with seasons, showing an increase in spring precipitation and a decrease in summer precipitation.

In this paper, the uncertainty of GCMs and the uncertainty of downscaling method in the process of climate change prediction for watershed precipitation will lead to the uncertainty of final results. The purpose of this paper is to reduce the uncertainty among climate models to a certain extent on the premise of maintaining the characteristics of climate models. However, only one downscaling method is adopted in this paper. In future studies, more evaluation indexes can be added and more downscaling methods can be used for comparison, so as to comprehensively analyze future climate change and reduce the uncertainty of simulation results.

References:

[1] CAO Y, ZHANG G H, LUO R T. Response of runoff and sediment discharge to global climate change in Jinghe River basin[J]. Science of Soil and Water Conservation, 2010, 8(2): 30-35. (in Chinese) DOI: 10.16843/j.sswc.2010.02.006.

[2] ZHOU T J. A robustness analysis of CMIP5 models over the east Asia-western north Pacific domain[J]. Engineering, 2017, 773-778. DOI: 10.1016/J.ENG.2017.05.018.

[3] ARNELL N W. Climate change and global water resources[J]. Global Environmental Change, 1999, 9(SI): 31-49.

[4] VARIS O, KAJANDER T, LEMMELA R. Climate and water: from climate models to water resources management and vice versa[J]. Climate Change, 2004, 66(3): 321-344.

[5] LIU C M, LIU W B, FU G B, et al. A discussion of some aspects of statistical downscaling in climate impacts assessment[J]. Progress in Water Science, 2012, 23(3): 427-437. (in Chinese) DOI: 10.14042/j.cnki.32.1309.2012.03.016.

[6] ROSANA N F, MARK R N, THOMAS M R. Climate change effects on summertime precipitation organization in the southeast United States[J]. Atmospheric Research, 2018(214): 348-363. DOI: 10.1016/j.atmosres.2018.08.012.

[7] LU G, JIE H, XINGWEI C, et al. Contributions of natural climate changes and human activities to the trend of extreme precipitation[J]. Atmospheric Research, 2018(205): 60-69. DOI: 10.1016/j.atmosres.2018.02.006.

[8] MEARNS L, BOGARDI I, GIORGI F, et al. Comparison of climate change scenarios generated from regional climate model experiments and statistical downscaling[J]. Journal of Geophysical Research-Atmospheres, 1999, 104(D6): 6603-6621.

[9] YANG X L, ZHENG W F, LING C Q, et al. Prediction of drought in the Yellow River based on statistical downscale study and SPI[J]. Journal of Hohai University (Natural Sciences), 2017, 45(5): 377-383. (in Chinese) DOI: 10.3876/j.issn.1000-1980.2017.05.001.

[10] HASAN D S, RATNAYAKE U, SHAMS S, et al. Prediction of climate change in Brunei Darussalam using statistical downscaling model[J]. Theoretical & Applied Climatology, 2018, 133(1-2): 343-360. DOI: 10.1007/s00704-017-2172-z.

[11] HUANG J, ZHANG J C, ZHANG Z X, et al. Estimation of future precipitation change in the Yangtze River basin by using statistical downscaling method[J]. Stochastic Environmental Research and Risk Assessment, 2011, 25(6): 781-792.

[12] LIU N, LI S L. Predicting summer rainfall over the Yangtze-Huai region based on time-scale decomposition statistical downscaling[J]. Weather and Forecasting, 2014, 29(1): 162-176. DOI: 10.1175/WAF-D-

13-00045.1

[13] CHEN P X, JIANG Z H, PENG D M. Multi-model statistical downscaling of spring precipitation simulation and projection in central Asia based on canonical correlation analysis[J]. Acta Meteorologica Sinica, 2017, 75(2): 236-247. (in Chinese) DOI: 10.11676/qxxb2017.017.

[14] LI Q L, WANG RK, DONG X T. Vegetation dynamics and its relationship with precipitation and runoff in upper Jinghe River basin[J]. Hydroelectric Power, 2015, 41(11): 21-33. (in Chinese) DOI: 10.3969/j.issn.0559-9342.2015.11.006.

[15] DUFRESNE J L, FOUJOLS M A, DENVIL S, et al. Climate change projections using the IPSL-CM5 earth system model: from CMIP3 to CMIP5[J]. Climate Dynamics, 2013, 40(9-10): 2123-2165. DOI: 10.1007/s00382-012-1636-1.

[16] SPERBER K R, ANNAMALAI H, KANG I S, et al. The Asian summer monsoon: an intercomparison of CMIP5 vs. CMIP3 simulations of the late 20th century[J]. Climate Dynamics, 2013, 41(9/10): 2711-2744. DOI: 10.1007/s00382-012-1607-6.

[17] FU G B, LIU Z F, CHARLES S P, et al. A score-based method for assessing the performance of GCMs: A case study of southeastern Australia[J]. Journal of Geophysical Research Atmospheres, 2013, 118(10): 4154-4167. DOI: 10.1002/jgrd.50269.

[18] CHEN S C, HUANG B S, WANG X G, et al. The precipitation characteristics and its evaluation and forecasting by general circulation models of CMIP5 at the Yanglou basin[J]. Pearl River, 2018, 39(6): 58-62, 97. (in Chinese) DOI: 10.3969/j.issn.1001-9235.2018.06.013.

[19] SEO K H, OK J. Assessing future changes in the east Asian summer monsoon using CMIP3 models: results from the best model ensemble[J]. Journal of Climate, 2013, 26(19): 7662-7675.

[20] MANN H B. Nonparametric test against trend[J]. Econometrica, 1945, 13(3): 245-259.

[21] KAHYA E, KALAYC S. Trend analysis of streamflow in Turkey[J]. Journal of Hydrology, 2004, 289(1-4): 128-144.

[22] FERRO C A, FRICKER T E. A bias-corrected decomposition of the brier score[J]. Quarterly Journal of Royal Meteorological Society, 2012, 138(668): 1954-1960.

[23] KNUTSON T R, DELWORTH T L, DIXON K W, et al. Model assessment of regional surface temperature trends(1949-1997)[J]. Journal of Geophysical Research, 1999, 104(24): 30981-30996.

[24] HAY L E, WILBY R L, LEAVESLEY G H. A comparison of delta change and downscaled GCM scenarios for three mountainous basins in the United States[J]. Jawra Journal of the American Water Resources Association, 2000, 36(2): 387-397.

[25] WILLBY R L, DAWSON C W, BARROW E M. SDSM 4.2: A decision support tool for the assessment of regional climate change impacts[J]. Environmental Modelling & Software, 2007, 145-157.

[26] MOHSEN A, HUSEYIN T. Future changes in maximum temperature using the statistical downscaling model(SDSM) at selected stations of Iran[J]. Modeling Earth Systems and Environment, 2016, 2(2): 2363-6203. DOI: 10.1007/s40808-016-0112-z.

[27] ZULKARNAIN H, SUPIAH S, SOBRI H. Application of SDSM and LARS-WG for simulating and downscaling of rainfall and temperature[J]. Theoretical and Applied Climatology, 2014, 116(1-2): 243-257. DOI: 10.1007/s00704-013-0951-8.

[28] DAI H H, YANG H B, HU Q F. Prediction of climate change over Shule River basin based on a statistical downscaling method[J]. Journal of Water Resources and Hydropower Engineering, 2015(5): 46-53. (in Chinese) DOI: 10.16198/j.cnki.1009-640X.2015.05.006.

[29] HAO Z C, SHI F X, WANG J H. Research and analysis of change of precipitation in headstream region of Yellow River by using statistical downscaling model[J]. Hydropower Energy Science, 2011(3): 1-4. (in Chinese)

[30] WEI F Y, HUANG J Y. A study of predictability for summer precipitation on east China using downscaleing techniques[J]. Tropical Meteorological Journal, 2010, 26(4): 483-490. (in Chinese)

[31] ZHAI W L, LI P J, LING K R. The prediction of climatic change and runoff response in the Dongjiang basin based on SDSM-SWAT model[J]. Pearl River, 2016, 37(4): 1-6. (in Chinese) DOI: 10.3969/j.issn.1001-9235.2016.04.001

[32] LIU W L, XIONG H L, LIU L N. Estimate of the climate change in Ganjiang River basin using SDSM method and CMIP5[J]. Soil and water conservation research, 2019, 26(2): 145-152. (in chinese) DOI: 10.13869/j.cnki.rswc.2019.02.021.

[33] LI W, JIANG Z H, XU J J. Extreme precipitation indices over China in CMIP5 models. Part II: probabilistic projection[J]. Journal of Climate, 2016, 29(24): 8989-9004. DOI: 10.1175/JCLI-D-16-0377.1.